

## Oscillations in laser direct writing of W from $\text{WCl}_6$ and $\text{H}_2$ : A theoretical analysis

N. Arnold, P.B. Kargl, R. Kullmer, D. Bäuerle

Angewandte Physik, Johannes-Kepler-Universität Linz, A-4040 Linz, Austria  
(Fax: +43-732/2468-9242; E-mail: NIKITA.ARNOLD@jk.uni.linz.ac.at)

Received: 14 May 1995/Accepted: 6 June 1995

**Abstract.** The origin of oscillations observed in laser direct writing of W lines on quartz substrates is studied on the basis of a one-dimensional model. The dependence of oscillations on laser power, scanning velocity, etc., is discussed. The predictions are compared with experimental data. The present approach can be applied also to other systems, where such oscillations have a different origin.

**PACS:** 42.62; 44.30; 61.80

Laser direct writing is a one-step technique for surface micropatterning. Different materials and precursor molecules were studied [1, 2]. Under certain conditions, oscillations in the height and width of lines are observed [1, 3–8]. The origin of these oscillations differs from system to system and sometimes remains speculative. Some of these oscillations were explained by latent heat effects [5], changes in the absorptivity with chemical composition [6, 9], temperature differences within deposits [10], etc. Different types of oscillations have been studied theoretically in [9–12]. Recently, we have developed a *one-dimensional* approach for laser direct writing [13] which also permits a description of oscillations [10]. In the present article, we extend these investigations with special emphasis on time-dependent effects observed with the deposition of W from  $\text{WCl}_6$  [7, 14]. Nevertheless, the model can be applied to other systems as well. The aim of the article is to provide a simple mathematical formalism which permits to understand qualitative features of the process.

### 1 Mathematical framework

Henceforth, we will employ the one-dimensional model for laser direct writing discussed in [10, 13]. When a metal is deposited onto a thermally insulating substrate where the ratio of thermal conductivities  $K^* = K_D/K_S \gg 1$ , the heat is transported mainly along the deposited stripe

(index D) and gradually dissipates into the substrate (index S). This allows to approximate the three-dimensional heat conduction problem by a one-dimensional equation for the temperature distribution along the stripe  $T(x, t)$ . In order to determine self-consistently the parameters of the stripe, such as its width  $2r$ , height  $h(x, t)$ , and distance  $a$  between the center of the laser beam and the front edge of the stripe, the heat equation must be solved together with the equation of growth. These equations can be written as [13]:

$$\frac{K_D}{D_D} F \frac{\partial T}{\partial t} = K_D \frac{\partial}{\partial x} \left( F \frac{\partial T}{\partial x} \right) - \eta K_S (T - T_0) + AP(x), \quad (1)$$

$$\frac{\partial h(x, t)}{\partial t} = W(x) + v_s \frac{\partial h(x, t)}{\partial x}, \quad (2)$$

where  $v_s$  is the scanning velocity,  $D_D$  the heat diffusivity,  $F \propto rh$  the cross section of lines,  $T_0$  the temperature of the surrounding,  $P(x)$  the laser power per unit length of the line, and  $A$  the absorptivity;  $\eta \approx 2$  characterizes heat losses into the substrate. Here, it has been assumed that the deposit is flat ( $h/r \ll 1$ ) and that the scanning term in (1) can be ignored. The growth rate can be described by the Arrhenius law

$$W(x) = W[T(x)] = k_0 \exp[-T_a/T(x)], \quad (3)$$

where  $T_a$  is the activation temperature and  $k_0$  the preexponential factor. To achieve further insight, we make additional simplifications: Firstly, we approximate partial differential equations by ordinary differential equations. We describe the hot area near the laser beam as a “chemical reactor” which is open with respect to mass and energy transfer. The chemical transformations result in the “production” of  $h$ , while the scanning term  $v_s \partial h(x, t)/\partial x$  removes the material from the reactor. Energy exchange is provided by the absorption of laser light and heat conduction. The reactor is characterized by the temperature of the zone near the center of the laser beam  $T_c$  and the (slowly varying) height  $h$  immediately behind the beam. For flat structures the changes in  $r$  and  $a$  are fast and we can assume  $r = r(h, T_c)$ . For each given value of

$h$  and laser power  $P$ , there exists a quasi-equilibrium value  $T_c = T_{c,eq}(h)$ . In other words,  $T_{c,eq}(h)$  is the temperature established by heat conduction in the artificially prepared stripe with height  $h$ . The function  $T_c = T_{c,eq}(h)$ , or rather the inverse function  $h = h_{eq}(T_c)$ , can be derived from (1) under different physical assumptions on the temperature at the edge of the line. We assume a temperature threshold for deposition  $T_{th}$  [14] and take into account the finite size of the laser focus  $w_0$ . This leads to the following equations [10]:

$$h_{eq}(T_c) = \frac{\sigma l^2}{K^* a} \quad (4)$$

with

$$\mu(T_c) = \text{arccosh}\left(\frac{\Delta T_c}{\Delta T_{th}}\right), l(T_c) = \frac{PA(T_c)}{\eta K_S \Delta T_{th}} e^{-\mu(T_c)},$$

$$a(T_c) = l\mu + \chi w_0, \quad (5)$$

where  $\Delta T = T - T_0$ ,  $\xi$ ,  $\chi$ , and  $\sigma$  are geometrical factors close to unity;  $l$  characterizes the decrease in laser-induced temperature along the  $x$ -direction.

After some perturbation, the temperature  $T_c$  of a stripe of height  $h$  shall return to the equilibrium value according to

$$\frac{dT_c}{dt} = \tau_T^{-1}(T_c, h) [T_{c,eq}(h) - T_c] = k_T(T_c, h) [h_{eq}(T_c) - h]. \quad (6)$$

The first square bracket determines the relation between the quasi-equilibrium temperature and  $h$ . The second expression is mathematically equivalent, but more convenient, since we can directly employ the dependence  $h_{eq}(T_c)$  given by (4, 5). The relaxation time  $\tau_T$  can be estimated as  $l^2/D_S$ . For the typical parameter values employed during the deposition of W in [7], we obtain from (4, 5)  $l^2 \approx hrK^* \approx 3 \times 10^{-4}$  cm, and  $\tau_T \approx 3 \times 10^{-2}$  s ( $D_S(\text{SiO}_2) \approx 10^{-2}$  cm<sup>2</sup>/s). When the expression in the square brackets is equal to zero,  $T_c$  remains constant, unless  $h$  changes due to deposition. With  $\partial h(x, t)/\partial x|_{x=0} \approx -h/\gamma a$  with  $\gamma \approx 1$ , we can approximate (2) by

$$\frac{dh}{dt} = W(T_c) - v_s \frac{h}{\gamma a(T_c)}. \quad (7)$$

The typical time constant for the changes in  $h$  is  $\tau_h \approx a/v_s \approx 10$  s. It is of the same order of magnitude as the observed oscillations. With overall equilibrium with respect to both heat conduction and growth,  $dT_c/dt = dh/dt = 0$ . This equilibrium situation and the influence of different parameters on  $h$ ,  $r$ , and  $T_c$  were studied in [10, 13].

The second simplification concerns the behavior of  $T_c$ . Because  $\tau_T \ll \tau_h$  in each moment,  $T_c$  can be calculated from the quasi-equilibrium temperature distribution  $T_c = T_{c,eq}(h)$ . Therefore, unless the expression in the brackets in (6) is close to zero, the (slow) variable  $h$  changes according to (7) with  $T_c = T_{c,eq}(h)$ . A rough estimation of the characteristic amplitudes of oscillations with  $\delta T \approx 10$ –100 K (theoretical estimation, Figs. 2, 4) and  $\delta h \approx 2 \times 10^{-4}$  cm (experimental observation, [7]) yields:  $k_T \approx \tau_T^{-1} \delta T/\delta h \approx 2 \times 10^6$ – $10^7$  K/cms. The exact value

of  $k_T$  is unimportant because  $T_c$  is the fast variable, i.e.,  $\tau_T \ll \tau_h$ .

## 2 Zero isoclines. Temperature dependent absorptivity

The oscillations observed during laser direct writing of W from  $\text{WCl}_6 + \text{H}_2$  cannot be explained on the basis of latent heat effects [7]. The estimated heat release  $Q\rho/MdV/dt \approx 6.2 \times 10^{-4}$  W ( $\rho \approx 19.3$  g/cm<sup>3</sup>, molar weight  $M \approx 184$  g/mole, deposition rate  $dV/dt \approx 10^{-8}$  cm<sup>3</sup>/s, and heat of reaction  $Q(298 \text{ K}) \approx 596$  kJ/mole [15]) can be ignored in comparison to the absorbed laser power (0.1–1 W). The oscillations can as well neither be attributed to changes in the heat conduction along a stripe of varying cross section [16] nor to transport limitations in the gas phase [12]. The latter would produce oscillations with periods of only  $t \approx r^2/D \approx 2.5 \times 10^{-6}$  s ( $r \approx 50$   $\mu\text{m}$ ,  $D \approx 10$  cm<sup>2</sup>/s [15]). Furthermore, with the growth rates observed in [7], the system is not strongly transport limited (with  $W \approx 1$   $\mu\text{m/s}$  and  $\rho_s/\rho_g \approx 4.7 \times 10^6$  for 0.5 mbar  $\text{WCl}_6$ , the dimensionless parameter becomes  $(\rho_s/\rho_g)Wr/D \approx 0.23$ ). A key in the interpretation of the oscillations are the changes in absorptivity  $A$ , observed experimentally [7].

In the visible, the absorptivity of pure W changes slightly with temperature. More important are changes in  $A$  related to changes in the morphology of W deposited at different temperatures, or different growth rates. These can be due to gas-phase and/or surface nucleation processes with subsequent changes in surface roughness [17].

However, because oscillations have been observed only in the presence of small amounts of oxygen [7], the most plausible explanation for the changes in  $A$  is the formation of  $\text{WO}_3$  on the surface of W lines.  $\text{WO}_3$  strongly absorbs 514.5 nm Ar<sup>+</sup>-laser radiation. It has a high rate of oxidation even at pressures around  $10^{-5}$  atm (up to  $10^{-3}$   $\mu\text{m/s}$  at temperatures around 1500 K) [18]. The equilibrium (with respect to oxidation-sublimation) value of the oxide layer thickness is a steep function of  $T$ . This can provide fast changes of  $A(T)$  from the value of pure W to the (much higher) value of  $\text{WO}_3$ . It may also explain the good localization of dark regions along the stripe [7].

Phenomenologically, we describe this behavior by a dependence of the absorptivity on temperature. Such a dependence, if strong enough, can lead to the appearance of oscillations.

The physical reasons are the following. Let us assume that  $A(T)$  increases with temperature faster than heat losses do. Then, if the temperature occasionally increases, the total energy input into the system increases. In this case,  $T$  continues to increase further if the laser power is kept constant. Later, extensive growth increases the cross section of the stripe to such an extent, that heat losses along the stripe exceed the absorbed power. As a consequence, the temperature drops again.

Within the relevant region (see below) the step-like increase in absorption observed in [7] can be described by

$$A(T) = A_0 + \frac{A_1}{\left[ \exp\left(\frac{T_A - T}{\delta T_A}\right) + 1 \right]}. \quad (8)$$

$\delta T_A$  is the width of the step in  $A$  at  $T_A$  and  $A_1$  its amplitude. Some comments are appropriate.

First, in [7], the absorptivity was measured as a function of the scanning velocity. The model suggests that there is a direct correspondence between  $v_S$  and  $T_c$  [10, 13]. Therefore, we have fitted the experimentally measured  $A(v_S)$  dependence by varying the coefficients in (8). The  $A(v_S)$  dependence was drawn in the same way as the dependence of  $r(v_S)$  and  $h(v_S)$  in [10, 13] with  $T_c$  as a parameter along the curves. It is clear from (4, 5) that an increase/decrease in  $A$  within a certain temperature interval will cause an increase/decrease in height and width of the stripe. It was confirmed in [7], that oscillations occur in an interval  $v_S$ , where the width and height of stripes increases dramatically. The  $A(v_S)$  dependence corresponding to the experimental data ([7], Fig. 6, upper curve) is shown in Fig. 1.

Second, the exact behavior of  $A(T)$ , in particular at low and high temperatures has almost no influence. Most important is the region, where the increase in  $A$  occurs, because it provides the non-monotonous behavior of the  $T_c$  zero isocline (see below). For this reason, we have chosen the relatively simple function (8), which does not describe the decrease in absorption at high scanning velocities, as observed in [7].

Third, the absorptivity may depend not only on temperature, but as well on the average roughness of the deposit which, in turn, depends on the growth rate  $W$ . However, with constant pressure of the precursor gas there is a direct correspondence between the growth rate and the temperature and such changes in  $A(T)$  are included in (8).

For the mathematical description of the oscillations we use the concept of zero isoclines [19]. In the case under consideration, the zero isoclines of  $h$  and  $T_c$  are the curves in the  $[h, T_c]$ -plane (phase plane) where the time derivatives of these variables are equal to zero (6, 7). Therefore, the  $T_c$  zero isocline is given by (4). It is shown by the dashed line in Fig. 2 for  $A = \text{const}$  and by solid line for  $A = A(T)$ . The  $h$  zero isocline (dash-dotted line) is given by

$$h(T_c) = \gamma \frac{a}{v_S} W(T_c). \quad (9)$$

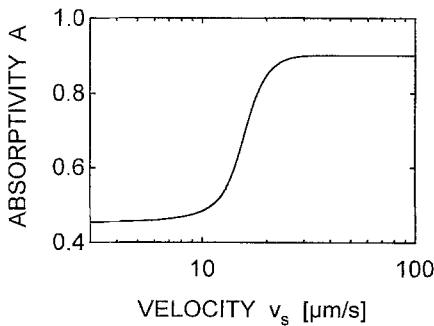


**Fig. 1.** Dependence of absorptivity  $A$  on the scanning velocity  $v_S$  as calculated from (8), (4, 5) and (9). The parameter values are:  $\eta = 1.6$ ,  $\xi = 1.25$ ,  $\gamma = 1.3$ ,  $\sigma = 0.962$ ,  $\chi = 1.0$ ,  $K_D = 8 \times 10^6$  erg/cm K,  $K_S = 3 \times 10^5$  erg/cm K,  $K^* = 26.6$ ,  $T_0 = 443$  K,  $T_{th} = 1200$  K,  $T_a = 2525$  K,  $k_0 = 1.6 \times 10^{-3}$  cm/s,  $w_0 = 7.5 \times 10^{-4}$  cm,  $P = 650$  mW,  $A_0 = 0.45$ ,  $A_1 = 0.45$ ,  $T_A = 1250$  K,  $\delta T_A = 10$  K

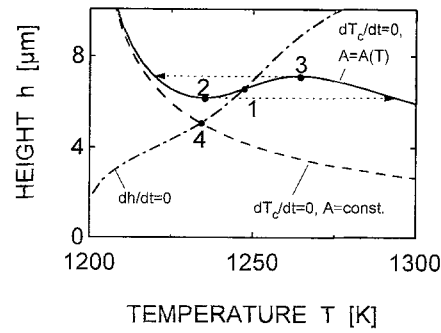


**Fig. 2.** Phase portrait of the deposition process in the  $[T_c, h]$ -plane (see text) calculated from (4, 5) and (9) with  $v_S = 1.5 \times 10^{-3}$  cm/s. Other parameters are the same as in Fig. 1. Dash-dotted curve:  $h$  zero isocline (9); dashed curve:  $T_c$  zero isocline (4) with  $A = \text{const}$  ( $A_1 = 0$ ); solid curve:  $T_c$  zero isocline with  $A(T)$  given by (8); 1, 4 are stationary points. Arrows indicate the limit cycle for  $A = A(T)$

The positions of the zero isoclines in the phase plane determine the qualitative behavior of the solution of (6, 7).

For  $A = \text{const}$ , the system first relaxes horizontally towards the  $T_c$  zero isocline (dashed line in Fig. 2) and then slowly approaches the equilibrium position 4, given by the intersection with the zero isocline for  $h$  (9). This equilibrium position is stable.

The  $T_c$  zero isocline for an absorptivity which increases with temperature is given by the solid curve. The evolution of the system is now quite different. First, it also relaxes to the  $T_c$  zero isocline, but cannot reach the equilibrium point 1, which is unstable. Thus, it jumps from one branch of solid curve to another at points 2 and 3, and the system ends up in a limit cycle, demonstrating an oscillatory behavior.

### 3 Conditions for the existence of oscillations

Oscillations occur, if the *only* equilibrium point 1 is placed between 2 and 3. These positions are given by zero derivatives of the right side of (4) with respect to  $T_c$ . From these conditions, we obtain the expressions for the slope of the  $A(T_c)$  function at these points:

$$\begin{aligned} \left. \frac{dA}{dT_c} \right|_{T_c=T_{2,3}} &= A(T_{2,3}) \left. \frac{d\mu}{dT_c} \right|_{T_c=T_{2,3}} \left( 1 + \frac{l}{l\mu + 2\chi w_0} \right) \\ &= \frac{A(T_{2,3})}{T_{2,3}} \frac{\left( 1 + \frac{l}{l\mu + 2\chi w_0} \right)}{\left( 1 - \Delta T_{th} / \Delta T_{2,3} \right)^{1/2}}. \end{aligned} \quad (10)$$

That means that the dependence  $A(T_c)$  in some temperature interval should necessarily be steeper than linear  $A \propto T_c$ , since the factor behind  $A/T$  in (10) always exceeds unity. This is the condition for a positive feedback. The energy input increases faster with temperature than heat losses. Note that oscillations were not observed when changes in  $A$  were not strong enough [7]. From Fig. 2 it is clear that the oscillations will occur if the  $h$  zero isocline (dash-dotted line) lies below the  $T_c$  zero isocline at

$T_c = T_2$  and above it at  $T_c = T_3$ , i.e., (4, 5) for:

$$\frac{W(T_2)}{v_s} < \frac{\sigma}{\gamma K^* a^2} \Big|_{T_c=T_2}, \text{ and } \frac{W(T_3)}{v_s} > \frac{\sigma}{\gamma K^* a^2} \Big|_{T_c=T_3}. \quad (11)$$

The region given by (11) is shown in Fig. 3 for the case of  $W$  deposited on quartz from  $WCl_6$  (full curves). The shaded area shows the experimentally determined dependence.

If only one of the conditions (1) is fulfilled, deposition is stable. If both inequalities are reversed, zero isoclines have three intersections, two of them are stable, the intermediate is a saddle point. This corresponds to the regime of bistability, when the system has two different stable regimes with all external parameters being the same.

However, because  $W(T_3) > W(T_2)$ , this requires the right side of (11) at  $T_3$  to be greater than at  $T_2$  which is possible only with an even stronger increase in absorptivity with temperature. Thus, oscillations and bistability can hardly be observed in the same system.

Let us simplify (11) for low and high laser powers. For low laser powers  $l\mu \ll \chi w_0$ , and expressions (10, 11) become dependent on the single parameter  $J$  only:

$$J = \frac{\sigma}{\gamma \chi^2} \frac{P^2}{K_D K_S w_0^2 k_0} v_s.$$

Thus, from (11) the region in the  $[P, v_s]$ -plane where oscillations occur is determined by:

$$C_1 v_s^{-1/2} < P < C_2 v_s^{-1/2}, \quad (12)$$

$C_1$  and  $C_2$  are constants. With increasing scanning velocity, the power interval for oscillations strongly decreases and can become experimentally unobservable.

With high laser powers  $l\mu \gg \chi w_0$ , and (4, 9) simplify to:

$$h(T_c) = \frac{\sigma P A(T_c)}{\eta K_D \Delta T_{th}} \mu^{-1} e^{-\mu}, \quad (13)$$

$$h(T_c) = \frac{\gamma P A(T_c)}{\eta K_S \Delta T_{th} v_s} \mu e^{-\mu} W(T_c). \quad (14)$$

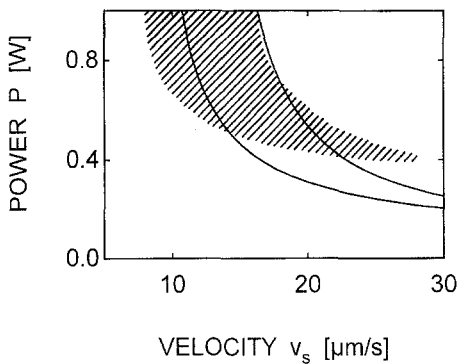


**Fig. 3.** Region of oscillations in the  $[P, v_s]$ -plane as calculated from (11). Parameters are the same as in Fig. 1. The shaded area indicates the region where oscillations have been observed experimentally for  $W$  deposition from  $WCl_6 + H_2$  [7]

The positions of  $T_{2,3}$  are given again by the zero derivative of the right side of (13), with respect to  $T_c$ , namely:

$$\frac{d}{dT_c} [\ln A(T_c)]_{T_c=T_{2,3}} = (\Delta T_c^2 - \Delta T_{th}^2)^{-1/2} \times [1 + \mu^{-1}(T_c)]_{T_c=T_{2,3}} \quad (15)$$

The condition (11) transforms to:

$$\mu^2(T_2) \exp\left(-\frac{T_a}{T_2}\right) < \frac{\sigma v_s K_S}{\gamma k_0 K_D} < \mu^2(T_3) \exp\left(-\frac{T_a}{T_3}\right). \quad (16)$$

The laser power does not enter these conditions. Thus, the region of oscillations in the  $[P, v_s]$ -plane for high powers is a band parallel to the  $P$  axis. This tendency is also revealed in the experimental results (Fig. 3).

#### 4 Dynamics of oscillations

In this section, we will show how oscillations depend on laser power and scanning velocity. The time-dependent behavior of the temperature  $T_c$  and height  $h$  can be obtained from (6, 7). A numerical solution is shown in Fig. 4. The width  $r = \xi a$  is calculated from (5). The laser power  $P = 650$  mW and the scanning velocity  $v_s = 15$   $\mu\text{m/s}$  correspond to values employed in [7]. The sharp initial increase in temperature is due to the small starting value of  $h$  and correspondingly small heat losses. This effect exists also in the experiments. One can see fast changes in temperature, corresponding to the jumps between the branches of the  $T_c$  zero isocline at points 2 and 3 (Fig. 2). The changes in height are smoother. The behavior of  $h$  and  $2r$  is in reasonable agreement with experimental values [7]. The main contribution to the temporal period of oscillations results from the time on the  $T_c$  zero isocline between jumps. It can be estimated analytically by integrating (7) along  $h = h_{eq}(T_c)$ . However, because of the complexity of the functions involved, it is easier to determine the period for different parameter sets directly from solutions as, e.g., the one depicted in Fig. 4.

The dependences of the spatial period  $\Lambda$  on  $v_s$  and  $P$  are shown in Fig. 5. Vertical lines (dashed) limit the regions where oscillations occur. Clearly,  $\Lambda$  was obtained

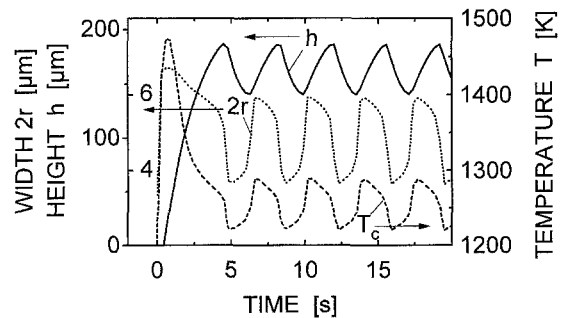


**Fig. 4.** Time-dependent behavior of the height (full curve, inner scale on left axis) and width  $d = 2r = 2\xi a$  of stripes (dotted curve, outer scale on the left axis) and the central temperature  $T_c$  (dashed curve). The parameters employed in (6, 7) were  $k_T = 2 \times 10^6$  K/cm s, initial conditions:  $T_c(0) = 1210$  K,  $h(0) = 1$   $\mu\text{m}$ . Other parameters are the same as in Fig. 1

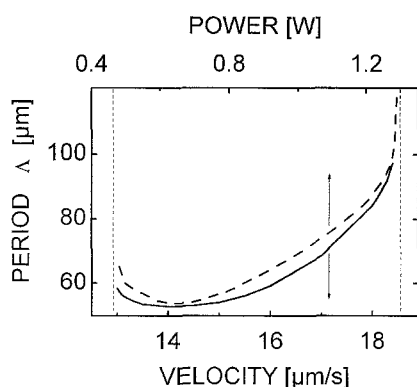


**Fig. 5.** Calculated dependences of the spatial period  $\Lambda$  on laser power  $P$  (dashed curve,  $v_s = 1.5 \times 10^{-3}$  cm/s) and scanning velocity  $v_s$  (solid curve,  $P = 650$  mW). The (vertical) dashed lines indicate borders of regions where oscillations occur

by multiplying the temporal period by  $v_s$ .  $\Lambda$  increases faster than linearly with both the laser power and the scanning velocity in almost all regions where oscillations exist. This is in agreement with the experimental observations. The experimental values of  $\Lambda$  [7] exceed the numerical ones by about a factor of 2. The significant increase in  $\Lambda$  at the borders is an artifact which is due to the approximations made. When the intersection point 1 (Fig. 2) is close to one of the extrema of the  $T_c$  zero isocline (points 2, 3), the approach based on only two differential equations becomes too crude and one has to consider the temperature distribution near the laser beam more accurately. When the parameters are beyond the range of the oscillations, but close to it, the model produces damped oscillations, as it was observed in the experiments.

The sensitivity of oscillations to the presence of hydrogen [7] can be tentatively attributed to two factors. First, as demonstrated in [14], the kinetic parameters of W deposition depend on hydrogen content. Thus, the position of the oscillatory region (Fig. 3) can change with hydrogen pressure, and the oscillations can disappear if other parameters are kept constant. Second, if oxidation proceeds in the transport-limited regime, the concentration of oxygen near the surface can decrease due to the decrease of the oxygen diffusion coefficient with increasing hydrogen pressure. Most probably, the oxidation kinetics also changes with hydrogen content.

## 5 Conclusions

It has been shown that the oscillations observed in laser direct writing of W lines on  $\text{SiO}_2$  substrates can be described on the basis of a one-dimensional approach. The laser powers and the scanning velocities at which oscilla-

tions exist, and their influence on the period of oscillations are estimated. The agreement with the experimental results is semiquantitative. In the W system, oscillations are due to an increase in absorptivity with temperature. However, the present approach can be applied to other systems as well. For example, the absorptivity of semi-transparent deposits can depend not only on temperature, but also on height  $h$ . If the latent heat of the reaction should be taken into account, the oscillatory shape of the zero isoclines can be provided by the additional heat-release term  $QW(T_c)$  in the right side of (6) rather than by the temperature-dependent absorptivity. In any case, the crucial point for the existence of oscillations is the non-monotonous shape of the zero isocline for the fast variable. For the problem discussed in the present article, the fast variable is the temperature near the center of the laser beam.

*Acknowledgements.* We wish to thank the "Jubiläumsfonds der österreichischen Nationalbank" for financial support and Prof. B. Luk'yanchuk for useful discussions and careful reading of the manuscript.

## References

1. D. Bäuerle: *Chemical Processing with Lasers*, Springer Ser. Mat. Sci. Vol. 1 (Springer, Berlin, Heidelberg, 1986)
2. D.J. Ehrlich, J.Y. Tsao (eds.): *Laser Microfabrication-Thin Film Processes and Lithography* (Academic, New York 1989)
3. S. Preuß, H. Stafast: *Appl. Phys. A* **54**, 152 (1992)
4. J. Messelhäuser, E.B. Flint, H. Suhr: *Appl. Phys. A* **55**, 196 (1992)
5. M.E. Gross, G.J. Fisanick, P.K. Gallagher, K.J. Schooes, M.D. Fennell: *Appl. Phys. Lett.* **47**, 923 (1985)
6. L. Baufay, M.E. Gross: In *Laser and Particle-Beam Chemical Processing for Microelectronics*, ed by D.J. Ehrlich, G.S. Higashi, M.M. Oprysko, MRS Symp. Proc. **101**, 89 (MRS, Pittsburgh, MA 1988)
7. P.B. Kargl, R. Kullmer, D. Bäuerle: *Appl. Phys. A* **57**, 175 (1993)
8. F. Foulon, M. Stuke: *Appl. Phys. A* **56**, 283 (1993)
9. P.E. Price Jr, K.F. Jensen: *Chem. Eng. Sci.* **44**, 1879 (1989)
10. N. Arnold, P.B. Kargl, D. Bäuerle: *Appl. Surf. Sci.* **86**, 457 (1995)
11. J. Han, K.F. Jensen: *J. Appl. Phys.* **75**, 2240 (1994)
12. N.V. Karlov, N.A. Kirichenko, B.S. Luk'yanchuk: *Laser Thermochemistry* (Nauka, Moscow 1992)
13. N. Arnold, R. Kullmer, D. Bäuerle: *Microelectron. Eng.* **20**, 31 (1993)
14. R. Kullmer, P.B. Kargl, D. Bäuerle: *Thin Solid Films* **218**, 122 (1992)
15. G. Dittmer, U. Niemann: *Philips Res. J.* **36**, 89 (1981)
16. N. Arnold, D. Bäuerle: *Microelectron. Eng.* **20**, 43 (1993)
17. E.G. Mehalchick, M.B. MacInnis: *Electrochem. Technol.* **6**, 66 (1968)
18. *Gmelin Handbuch der Anorganischen Chemie*: W. Wolfram, Tungsten, Suppl. B1, Suppl. B2 (Springer, Berlin, Heidelberg 1979) p. 161
19. A.A. Andronov, A.A. Vitt, S.E. Khaikin: *Theory of Oscillations* (Nauka, Moscow 1981)